A peer-reviewed version of this preprint was published in PeerJ on 1 September 2015.

View the peer-reviewed version (peerj.com/articles/1213), which is the preferred citable publication unless you specifically need to cite this preprint.

Chughtai AA, Kaššák F, Kostrouchová M, Novotný JP, Krause MW, Saudek V, Kostrouch Z, Kostrouchová M. 2015. Perilipin-related protein regulates lipid metabolism in *C. elegans*. PeerJ 3:e1213 https://doi.org/10.7717/peerj.1213

Perilipin-related protein regulates lipid metabolism in *C. elegans*

Ahmed A. Chughtai, Filip Kaššák, Markéta Kostrouchová, Jan P. Novotný, Michael W. Krause, Vladimír Saudek, Zdenek Kostrouch, Marta Kostrouchová

The perilipins are lipid droplet surface proteins that contribute to fat metabolism by controlling the access of lipids to lipolytic enzymes. Perilipins have been identified in organisms as diverse as metazoa, fungi, and amoebas but strikingly not in nematodes. Here we identify the protein encoded by the *W01A8.1* gene in *Caenorhabditis elegans* as the closest homologue of metazoan perilipin. We demonstrate that nematode W01A8.1 is a cytoplasmic protein residing on lipid droplets. Human perilipins 1 and 2 localize in transgenic *C. elegans* on the same structures as proteins expressed from W01A8.1 gene. Inhibition and elimination of W01A8.1 affects the appearance of lipid droplets especially visible as the formation of large lipid droplets localized around the dividing nucleus during the early zygotic divisions. This phenomenon disappears in later stages of embryogenesis indicating the existence of an additional mechanism of lipid regulation in *C. elegans*. Our results demonstrate that perilipin-related regulation of fat metabolism is conserved in nematodes and provide new possibilities for functional studies of lipid metabolism.

Perilipin-related protein regulates lipid metabolism in *C. elegans*

Ahmed Ali Chughtai[1,2], Filip Kaššák[1,2], Markéta Kostrouchová[1,2], Jan Philipp Novotný[1,2], Michael W. Krause[3], Vladimír Saudek[4,#], Zdenek Kostrouch[1,2] and Marta Kostrouchová[1,2,*]

1 Charles University in Prague, First Faculty of Medicine, Institute of Cellular Biology and Pathology, Kateřinská 32, 128 00 Prague 2, Czech Republic

2 Laboratory of Molecular Biology and Genetics, and Laboratory of Molecular Pathology, Program 5.2.4., Biocev, City Point, Hvězdova 1689/2a, 140 62 Prague 4, Czech Republic

3 Laboratory of Molecular Biology, National Institute of Diabetes and Digestive and Kidney Diseases, National Institutes of Health, Bethesda, Maryland, USA

4 University of Cambridge Metabolic Research Laboratories, Wellcome Trust–Medical Research Council Institute of Metabolic Science, Cambridge CB2 0QQ, United Kingdom

[*] Corresponding author

[#] Corresponding author for bioinformatics

[*] Address for correspondence: Marta Kostrouchová, Laboratory of Molecular Biology and Genetics, Institute of Cellular Biology and Pathology, First Faculty of Medicine, Ke Karlovu 2, 128 00 Prague 2, Czech Republic. Email: marta.kostrouchova@lf1.cuni.cz

[#] Address for correspondence concerning bioinformatics: Vladimir Saudek, email: vladimir.saudek@gmail.com

25 **Running title:** Perilipin homologue in *C. elegans*

Abstract

The perilipins are lipid droplet surface proteins that contribute to fat metabolism by controlling the access of lipids to lipolytic enzymes. Perilipins have been identified in organisms as diverse as metazoa, fungi, and amoebas but strikingly not in nematodes. Here we identify the protein encoded by the *W01A8.1* gene in *Caenorhabditis elegans* as the closest homologue of metazoan perilipin. We demonstrate that nematode W01A8.1 is a cytoplasmic protein residing on lipid droplets. Human perilipins 1 and 2 localize in transgenic *Caenorhabditis elegans* on the same structures as proteins expressed from *W01A8.1* gene. Inhibition and elimination of *W01A8.1* affects the appearance of lipid droplets especially visible as the formation of large lipid droplets localized around the dividing nucleus during the early zygotic divisions. This phenomenon disappears in later stages of embryogenesis indicating the existence of an additional mechanism of lipid regulation in *C. elegans*. Our results demonstrate that perilipin-related regulation of fat metabolism is conserved in nematodes and provide new possibilities for functional studies of lipid metabolism.

Keywords *Caenorhabditis elegans*, perilipin, lipid droplets, fat metabolism, perilipin-related protein in *C. elegans*

Abbreviations

LD – lipid droplet, *W01A8.1* – cosmid gene name, *W01A8.1(a, b*, or *c*) – transcript isoforms encoded by *W01A8.1*, W01A8.1(a, b, or c) – proteins encoded by corresponding transcripts, W01A8.1 – any protein encoded by *W01A8.1*

Introduction

Central to the understanding of fat metabolism are fat storage organelles, or lipid droplets (LDs), present in the cytoplasm of all metazoans. Perilipins, encoded in mammals by the *PLIN* genes, belong to a well-conserved family of PAT proteins (Lu et al. 2001) that are targeted to LD surfaces and regulate lipid storage and hydrolysis by regulating the access of various proteins to stored fat (Brasaemle 2007). Functional PLIN proteins (Lu et al. 2001) have been identified in evolutionarily diverse organisms such as *Drosophila* (Teixeira et al. 2003), *Dictyostelium* (Du et al. 2013) and fungi (Wang & St Leger 2007) and protein databases list clear orthologues in diverse, non-plant eukaryota, including the simplest metazoan *Trichoplax adherens*, sponges, crustaceans, and choanoflagelates (UniProt proteins B3RRM2, I1GA14, G5DCP6, F2UJD9, respectively). In humans and other mammals, the PLIN family consists of five members (Kimmel et al. 2010) (Perilipin 1 to 5) with diverse tissue distribution, specificity, and partially redundant functions. Strikingly, no perilipin othologue has been identified in *C. elegans*, suggesting that nematode-specific lipid regulatory pathways might exist in this phylum and perhaps in others as well.

This unusual evolutionary gap in the perilipins prompted us to re-examine the *C. elegans* genome for a gene related to mammalian perilipin. We identify *W01A8.1* as the likely *C. elegans* orthologue of mammalian perilipin genes. We show that W01A8.1 is the previously unrecognized *C. elegans* homologue of vertebrate perilipins that possesses all functional domains characteristic for perilipins and functions in lipid metabolism at the level of lipid droplets.

The protein encoded by this gene (W01A8.1) is identified as Mediator Complex subunit 28 (MDT-28) in many protein databases (e.g. Pfam, UniProt, PIR, WormPep) (accessed on March 14, 2015), but the bioinformatics analysis reveals that this is a mis-annotation. We observe that protein isoforms expressed from *W01A8.1* are cytoplasmic proteins, residing predominantly on membranous

structures of enterocytes and epidermal cells that have the characteristics of lipid droplets. We also show that transgene-encoded GFP fusion proteins of human Perilipins 1 and 2 localize in *C. elegans* similarly as W01A8.1::GFP on vesicular structures that are positive for lipid content. Furthermore, inhibition or elimination of *W01A8.1* leads to altered appearance and behavior of lipid droplets most prominent in the germline and in early embryos. We also show that *C. elegans* can compensate for the loss of *W01A8.1* in all developmental stages except very early embryos by an additional fat degradation mechanism. This discovery offers promising possibilities for functional studies of lipid metabolism in a nematode model system.

Materials and methods

Sequence analysis

Perilipin orthologues and W01A8.1 sequences were extracted from UniProt, NCBI and OMA (omabrowser.org) databases. Chordate and nematode sequences were aligned separately using the T-Coffee algorithm (Notredame, Higgins & Heringa 2000) (server tcoffee.crg.cat) and submitted to PSI-BLAST (Altschul et al. 1997) (E-value inclusion threshold < 10^{-3}, 5 iterations) and HHpred (Remmert et al. 2011; Biegert & Soding 2008). searches as implemented in MPItoolkit (toolkit.tuebingen.mpg.de). Repeat detection used HHrepID module in MPItoolkit. Alignments were displayed and analyzed in Jalview app (jalview.org).

Strains, transgenic lines and genome editing

Wild type animals, N2 (var. Bristol), were used unless otherwise noted and all strains were maintained as described (Brenner 1974). Transgenic lines were prepared using microinjections into gonads of young adult N2 hermaphrodites as described (Tabara et al. 1999; Timmons, Court & Fire

2001; Vohanka et al. 2010). All injections also included mCherry co-injection markers: pCFJ90, pCJ104 and pGH8 (Dickinson et al. 2013).

To create mutants, we employed CRISPR/Cas9 system as described (Dickinson et al. 2013). The following plasmids were constructed: pCK001 targeting the sgRNA (+323) to the second exon of the *W01A8.1* gene (forward primer #7992), and pCK023 targeting the sgRNA (+1372) to the sixth exon (forward primer #8078). The reverse primer was #7993. A scheme of known expressed isoforms listed in Wormbase WS246 and the strategy for the disruption of *W01A8.1* gene is shown in Supplementary Fig. S1 and Supplementary Fig. S2. Primers used in this study are listed in Supplementary Table S1.

The following transgenic lines regulated by *W01A8.1* natural promoter were prepared: *W01A8.1a/c::gfp* and *W01A8.1b::gfp* (containing the whole coding sequence of isoforms a and b). *W01A8.1* isoforms a and c have identical 3' ends which both could be expressed from *W01A8.1a/c::gfp*. This construct also includes complete untagged isoform b. The GFP-tagged isoform a (plasmid pCK28 {$P_{W01A8.1}$*::W01A8.1(a)synth::gfp::unc-54 3' UTR*}) was constructed by synthesizing the *W01A8.1a* sequence with modified codons to allow protection from CRISPR/Cas9 targeted sgRNA and prepared as a GeneArt® Strings™ DNA Fragment from Invitrogen (Invitrogen, Carlsbad, Ca, USA) and cloned using GeneArt® Seamless Cloning System (Invitrogen) into pPD95.75(NeoR). Schemes for isoforms expressed from *W01A8.1* gene and preparation of GFP tagged transgenes are given in Supplementary Figs. S1 and S2.

Human *PLIN2* and *PLIN3* were cloned from a collection of anonymous unmarked samples (*PLIN2*), and from human peripheral lymphocytes (*PLIN3*) donated by a volunteer with a written consent in compliance with the legislation of the Czech Republic and European Union (Act No 372/2011 of 11. 11. 2011 on Health Care Services, Coll., Paragraph 81, section 1a and section 4a,

which is in accordance with the declaration of Helsinki and was approved by the Ethical Committee of the First Faculty of Medicine, Charles University in Prague).

Human *PLIN1* was prepared as a synthetic construct coding for PLIN1, using codons differing as much as possible from wild type *PLIN1* at the DNA level (Invitrogen - ThermoFischer Scientific, Waltham, Massachusetts, USA) and cloned into the GFP vector pPD95.75(NeoR) using the same approach as synthetic *W01A8.1a*.

Transgenic lines expressing human *PLIN1*, *PLIN2*, *PLIN3* tagged by GFP under *W01A8.1* natural promoter were prepared using N2 animals and animals with disrupted *W01A8.1*.

Inhibition of gene expression by RNA interference

Inhibition of *W01A8.1* expression used the RNAi protocol of injections of dsRNA into gonads of young adult hermaphrodites as well as RNAi through feeding animals bacteria producing dsRNA as previously described (Tabara et al. 1999; Timmons, Court & Fire 2001; Vohanka et al. 2010).

Injection RNAi Protocol

Double stranded RNA (dsRNA) was prepared for injection by in vitro transcription reactions (SP6/T7 Riboprobe® in vitro Transcription Systems, Promega, Madison, WI, USA) from opposing promoters with each single stranded RNA (ssRNA). For RNAi directed against *W01A8.1*, BamHI or ApaI linearized pCK014 plasmid preparations were used in separate reactions to generate complementary ssRNA. After linearization the DNA was phenol-chloroform extracted and ethanol precipitated. BamHI linearized DNA was transcribed using T7 RNA Polymerase while ApaI linearized DNA with SP6 RNA Polymerase. After in vitro transcription (~2 hours) equal volumes of sense and antisense RNA were incubated at 75°C for 10 min and then cooled at room temperature for 30 min. Control RNAi was prepared from the promoter region of *nhr-60* as previously described (Simeckova et

al. 2007). The dsRNA concentration was measured using a UV spectrophotometer and ~1 µg/µl was used for injections.

Feeding RNAi Protocol

Nematode Growth Medium (NGM) agar plates were prepared according to standard protocols and were supplemented with Ampicillin (100µg/ml final concentration) and isopropyl β-D-1-thiogalactopyranoside (IPTG) (1.5mM final concentration). *E. coli* strain HT115 was transformed with pCK015 and control L4440 vector. After transformation, a single colony from each was used to inoculate LB medium with Ampicillin (100µg/ml final concentration). The culture was grown to OD_{600} ≈ 1.0 and poured onto NGM agar plates to completely cover the surface and excess was removed. The bacteria were allowed to grow and were induced overnight at room temperate (~22°C).

Fecundity and brood size assay

Fecundity measurement following RNAi (injection method) was conducted using a total of 50 young adult worms (25 control and 25 inhibited by RNAi specific for *W01A8.1*). Brood size assay was performed for *W01A8.1* disrupted animals and controls (n=15 for each group). The progeny was determined during 6 days.

RNA isolation

Total RNA was isolated as described and the quality of samples was assessed using agarose gel electrophoresis and spectrophotometrically (Vohanka et al. 2010).

Single worm PCR

Single animals were placed into 5µl of worm lysis buffer (10mM Tris-HCl pH8.3, 50mM KCl,

2.5mM MgCl2, 0.45% NP-40, 0.45% Tween 20, 0.0% Gelatin and 500ug/ml fresh proteinase K) in a PCR tube. Animals were frozen at -80°C for 5 min before placing the tube into a thermal cycler and run under the following conditions: heat to 60°C for 60 min followed by inactivation of proteinase K by heating to 95°C for 20 min. Post-lysis, a PCR reaction mix (45µl) targeting the template of choice was added and cycled for ~35 times with Q5® Hot Start DNA polymerase (New England Biolabs).

LipidTox staining

The lipid staining protocol was done as described (O'Rourke et al. 2009) with modifications. Approximately 200 to 500 animals were harvested from NGM plates with 1X PBS and washed several times to remove *E. coli* and pelleted at 1,500g. To the pellet, 500 µl 2X MRWB (160 mM KCl, 40 mM NaCl, 14 mM Na2EGTA, 1 mM Spermidine 3HCl, 0.4 mM Spermine, 30 mM NaPIPES pH 7.4, 0.2% beta-ME) and 100 µl 20%paraformaldehyde were added and the volume was adjusted up to 1ml with 1X PBS. Inverting the tube several times mixed the worms in solution after which it was allowed to fix for ~60 min at room temperature with gentle shaking.

After fixation, animals were pelleted at 1,500g and washed 3 times with 1 ml Tris-HCl buffer (100 mM, pH 7.4). After the third wash, the supernatant was discarded down to 100µl and 650µl of Tris-HCL buffer was added followed by 250µl of fresh/frozen reduction buffer (100 mM Tris-Cl pH 7.4, 40 mM DTT). Worms were then left shaking for ~30 min at room temperature. After reduction, worms were washed as before 3 times in 1X PBS. After the final PBS wash, the volume was brought up to 500µl and then 500µl of LipidTox (Red) (1:500 dilution) (Invitrogen) was added to make a final volume of 1ml. The final concentration of 1:1000 dilution of LipidTox was used. The worms were left in the dark for at least 60 min with shaking before viewing.

In vivo and after fixation Nile red staining protocols were done as described (Barros et al. 2012; O'Rourke & Ruvkun 2013).

Microinjections

Microinjections of plasmids, DNA amplicons or dsRNA into gonads of young adult hermaphrodites were done using an Olympus IX70 microscope equipped with a Narishige microinjection system (Olympus, Tokyo, Japan).

Microscopy

Fluorescence microscopy and Nomarski optics microscopy were done using an Olympus BX60 microscope equipped with DP30BW CD camera (Olympus, Tokyo, Japan).

Results

Identification of a perilipin orthologue in *C. elegans*

We performed BLASTp searches with individual protein sequences of human perilipins that generated no significant hits to Nematoda sequences in the UniProt database, consistent with previous efforts that failed to identify a perilipin-related protein in this phylum. However, when a sequence alignment of chordate perilipins 2 and 3 (OMA database) was submitted as query in PSI-BLAST, the *C. elegans* protein W01A8.1a (Q23095_CAEEL) was identified as a highly significant hit ($E=3x10^{-13}$). A reciprocal PSI-BLAST search with the aligned closest nematode homologues of W01A8.1a identified chordate perilipins as strong hits with human Perilipin 2 (significance score $E=10^{-53}$) appearing in the second iteration of the search. Similarly, HHpred profile-to-profile searches with human perilipin sequences as a query of the *C. elegans* proteome identified proteins coded by W01A8.1 (a, b or c) and reciprocally W01A8.1a showed profile homology to all human perilipins and the corresponding Pfam (Punta et al. 2012) perilipin profile (PF03036). Each available nematode proteome contained only a single such perilipin-related sequence, in stark contrast to the chordates

proteomes that had 2 to 5 perilipin paralogues. A sequence alignment of Plin2 and 3 from two selected vertebrates is compared with their nematode homologues (Fig. 1).

The alignment encompasses a substantial part of *C. elegans* and human sequences (e.g. 90% of W01A8.1 and 87% of Perilipin 2) and covers all three domains characteristic for perilipins (N-terminal PAT, imperfect amphiphilic 11-mer repeat (Brasaemle 2007) and C-terminal four-helix bundle (Hickenbottom et al. 2004)) covering approximately amino acids 10-100, 125-190 and 220-380 respectively in W01A8.1a. As W01A8.1 and human perilipins appear to be the best mutual reciprocal PSI-BLAST and HHpred hits, W01A8.1 is a very good candidate for a *C. elegans* orthologue of perilipin.

Protein databases annotate W01A8.1 as Mediator Complex subunit 28, hence the official protein name assignment of MDT-28 in WormBase (WS246). Pfam database (Punta et al. 2012) based the Mediator 28 Hidden Markov model profile on a seed alignment of bovine and mosquito Mediator 28 sequences with W01A8.1. This very profile was probably used subsequently in all automatic annotations of the nematode sequences. However, no substantial homology between W01A8.1 and Mediator 28 exists as shown in the above searches. Since using the WormBase name of W01A8.1 (MDT-28) would be misleading, the gene is referred here by the cosmid name *W01A8.1*, which gives rise to at least three protein isoforms designated W01A8.1a, W01A8.1b, and W01A8.1c from at least seven different transcripts (*W01A8.1a.1*, *W01A8.1a.2*, *W01A8.1b.1*, *W01A8.1b.2*, *W01A8.1b.3*, *W01A8.1c.1*, *W01A8.1c.2*). The three protein isoforms are 415, 385, and 418 amino acid residues in length for isoform a, b, and c, respectively (Supplementary Fig. S1). According to the *C. elegans* nomenclature, we suggest to rename *W01A8.1* as *Cel-plin-1* (isoform a, b, and c) and proteins Cel-PLIN-1 (isoform a, b, and c).

W01A8.1 protein products are cytoplasmic and reside primarily on lipid droplets

If the proteins encoded by *W01A8.1* act as perilipins, they would be expected to be associated with lipid droplets. To test this, we created translational reporter transgenes regulated by the putative endogenous promoter expressing isoform b and lines in which the genomic locus was tagged by an in-frame C-terminal GFP cassette. The second transgene, *W01A8.1a/c::gfp*, is likely to express not only high levels of a and c tagged isoforms, but also the native isoform b (Supplementary Fig. S1). The translational fusion constructs resulted in high levels of cytoplasmic proteins present in intestinal and epidermal cells on vesicular structures with the characteristic appearance of lipid droplets. This pattern of expression and cellular distribution was observed beginning at the three-fold embryonic stage and continued throughout development to adulthood (Fig. 2). To confirm that the observed GFP-associated vesicular structures were indeed lipid droplets, transgenic animals were stained with the lipophilic reagent LipidTox as previously described (O'Rourke et al. 2009). The translational GFP fusion protein reporters were localized at the periphery of fat droplets that were LipidTox positive (Fig. 2). The animals expressing W01A8.1a/c::GFP had generally low fat content, keeping with the expected overexpression of the native isoform b from this transgene. We also noted that animals with high levels of W01A8.1a/c::GFP had an altered morphology of the gonad and embryos.

Human PLINs 1and 2 label identical compartments as W01A8.1 proteins in *C. elegans*

We prepared transgenic *C. elegans* lines expressing human PLIN1, PLIN2 and PLIN3 fused to GFP and regulated by the *W01A8.1* promoter. PLIN1::GFP and PLIN2::GFP were localized on spherical cytoplasmic structures primarily in gut and epidermal cells (Fig. 3A, C, D and F) with identical appearance as W01A8.1 translational reporter GFP tagged proteins and *Drosophila* PLIN1::GFP expressed in *C. elegans* as reported by Liu et al. (Liu et al. 2014). PLIN3 expression was

diffusely cytoplasmic and only faintly defined spherical structures (Fig. 3G and I). The structures clearly labeled with PLIN1::GFP and PLIN2::GFP were also positive in LipidTox staining (shown for PLIN2::GFP in Fig. 3J, K and L). We conclude that W01A8 proteins are localized on the same structures as human PLIN1 and PLIN2.

W01A8.1 reduction-of-function causes reduction of brood size, and alters the appearance of lipid droplets in early embryos

To test the function of *W01A8.1*, we used RNAi done by germline injection and by feeding. *W01A8.1* RNAi resulted in a significantly smaller brood size, with approximately 1/3 less progeny from hermaphrodites injected with dsRNA compared to controls (n = 260, n = 550, for the day one and n = 1000, n = 1400 for the day two). Repetition of knock-down by RNAi feeding over two generations confirmed this observation (Supplementary Fig. S3). Staining of adult hermaphrodites with LipidTox (after formaldehyde fixation) revealed larger lipid droplets in early embryos derived from adults inhibited for *W01A8.1* (Fig. 4A and B) compared to controls (Fig. 4C and D).

Targeted disruption of *W01A8.1* results in early embryonic defects but not lethality

In order to eliminate the W01A8.1 function completely, we designed a CRISPR/Cas9-mediated genome edit to eliminate almost the entire coding region (Supplementary Fig. S2). We also included a rescuing plasmid consisting of isoform a that was prepared as cDNA synthesized in vitro using synonymous codons (*W01A8.1(a)synth::gfp*) that is protected against CRISPR/Cas9 targeted editing but allows the expression of wild type isoform a at the protein level. Strains with high levels of W01A8.1(a)synth::GFP exhibited gonad anomalies and low brood size. However, lines that expressed low quantities of the GFP fusion transgene were morphologically normal and W01A8.1(a)synth::GFP

was found on lipid droplet-like structures as expected (Fig. 4E and G) that also stained positive by LipidTox (Fig. 4F and G). This transgenic strain yielded lines either carrying or losing the rescuing transgene in the background of a disrupted endogenous *W01A8.1*. Surprisingly, animals with the deleted *W01A8.1* locus that lost the extra-chromosomal rescuing array were able to reproduce normally. From several lines that had confirmed disruption of *W01A8.1* and confirmed loss of the extrachromosomal potentially balancing array, the line CK123 (KV001) was used for subsequent analyses. As was observed in *W01A8.1* RNAi embryos, loss of *W01A8.1* activity resulted in the formation of large LipidTox-positive structures (Fig. 4H and I) that were clearly bigger than droplets observed in control embryos. These large lipid-containing structures were observable in fixed, but unstained embryos as well as in live mutant embryos using Nomarski optics (Fig. 5I) and were stained by LipidTox but were not seen in control N2 embryos (Fig. 5J). Viewing through multiple focal planes in live, developing embryos lacking *W01A8.1* showed that these large lipid droplets are present in embryos during the early mitotic divisions and were localized around the nucleus. Staining with LipidTox confirmed the lipid content in the vesicular structures arranged around dividing nucleus (Fig. 4 M).

These large vesicles persist through the two-cell stage, disappearing in most embryos with more than 6 cells. On fixed, freeze-cracked embryos stained with LipidTox, larger than wild type lipid droplets are visible until late embryonic stages, including three fold embryos. Brood size assay of the *W01A8.1* null mutant strain revealed a ~10% decrease in the total number of progeny compared with wild type controls (Supplementary Fig. S4).

Discussion

Lipolysis is a tightly regulated cellular process in which triacylglycerol fatty acids (TAG) are degraded into free fatty acids (FFA) and glycerol (G) with intermediates of diacylglycerol (DAG) and monoacylglycerol (MAG). The function and regulation of three key lipases (adipose triglyceride lipase (ATGL), hormone-sensitive lipase (HSL) and monoglyceride lipase (MGL)) have been studied in great detail in mammalian adipocytes (reviewed in (Lass et al. 2011)). Multidomain and multifunctional LD coating proteins, the perilipins, mediate the access of ATGL and HSL to LDs. Briefly (Fig. 5), the phosphorylated N-terminal domain PAT in perilipin interacts with HSL and brings it in contact with lipid droplets (LDs) (Shen et al. 2009). At the same time, the C-terminal phosphorylation (controlled by the kinase PKA) releases a specific activator of ATGL named ABHD5 without which ATGL remains inactive in the cytoplasm. The final step of the glycolysis is catalyzed by MGL. Conversely, unphosphorylated perilipin blocks lipolysis in the basal fed state by blocking the access of lipolytic enzymes to the fat stored in LDs. Both HSL and ATGL are the rate-limiting enzymes needed for fatty acids mobilization (Schweiger et al. 2006). A variation of this regulatory process, although less well understood in detail, exists in other cells and organisms. Most organisms so far studied contain several perilipin genes, complicating the analysis of complete perilipin loss-of-function.

Clear orthologues of ATGL, HSL, MGL, ABHD5 and catalytic and regulatory subunits of PKA have been identified in *C. elegans* (ATGL-1, HOSL-1, LID-1, KIN-1, KIN-2 respectively (Lee et al. 2014) (Fig. 5). The MGL orthologue remains to be identified but several un-annotated homologous proteins exist (Birsoy, Festuccia & Laplante 2013). A recent careful and elegant study of ATGL function and regulation (Lee et al. 2014) revealed that the process in *C. elegans* was almost identical to that found in mammalian adipocytes. Even the degradation of ABHD5 in the proteasome (Dai et al. 2013) is mirrored in *C. elegans* (Lee et al. 2014). The glaring difference in fat storage and metabolism seemed to be the absence of perilipin in nematode genomes.

Here we have established that *C. elegans* possesses a close homologue of perilipin that is intimately involved in the regulation of lipid metabolism. Although the sequence alignment of *C. elegans* and human homologues of perilipin does not appear visually very informative (Fig. 1), the underlying evolutionary conserved homology is statistically very significant. Perilipin is a scaffolding protein allowing co-evolution of interacting domains and divergence of non-docking sequences. Thus the function can be conserved even with limited amino acid conservation across species. This evolutionary plasticity was already apparent in the alignment of the human perilipin paralogues where only the knowledge of the three dimensional structure enabled observations of the similarities in the C-terminal domains (Hickenbottom et al. 2004). The nematode sequences have diverged beyond the point where pairwise comparisons used in routine searches can reveal homology, hence the difficulty in identifying the nematode orthologues. Only rigorous statistical analysis of the hidden Markov profiles of a great number of diverse sequences made it possible to identify the conserved domain composition.

The nematode perilipin-related protein W01A8.1 contains all three major perilipin features: N-terminal PAT domain, amphipathic region composed of imperfect helical repeats and C-terminal apolipoprotein-like four-helix bundle. In mammals, the first two domains are known to be responsible for the interaction with HSL and LDs respectively and the ATGL interaction region resides in the C-

terminus following the bundle. The function of the bundle is still unclear but its stability probably fine-tunes the solubility and the affinity to LDs (Brasaemle 2007). All these functions will have to be investigated in the isoforms of W01A8.1 in the future. The repeats are confirmed by analysis of internal homology using the HHrepID algorithm and the helical composition by secondary structure prediction. The bundle appears not to be stabilized by β-sheets as in human Perilipin 3 as revealed by the absence of the homology in the C-terminal region. The β-sheets are similarly absent in Perilipin 1.

Our findings are consistent with a proteomic study that found that W01A8.1b is among the most abundant proteins associated with LDs (Zhang et al. 2012). Similarly, perilipins are abundant proteins on mammalian LDs, although the distribution and proportion of the individual isoforms changes depending on the cell type and metabolic state (Brasaemle et al. 2004). Perilipins are widely used as general markers of LDs and it seems that W01A8.1a or b can be exploited for the same purposes; human PLIN1 was recently proposed as a marker for LDs in *C. elegans* (Liu et al. 2014).

Our study points at possible problems with gene denomination. Renaming genes may be warranted if new data show need for it. However, gene names once attributed cannot be removed from databases since the data deposited in databases are likely to be incorporated in numerous meta-analyses, publications or secondary databases through automatic annotations. Gene names related to predicted proteins based on low level of sequence similarity without additional functional data may lead to classification problems. In such cases, before a wide consensus on the function of the particular gene and derived proteins is reached, the genetic cosmid-based nomenclature may be preferable.

Surprisingly, in laboratory conditions *C. elegans* can overcome the complete loss of the perilipin-related protein W01A8.1, presumably by activating perilipin-independent lipid degradation. Previous work has shown that an additional lipid degradation pathway, autophagy, was important for lipid metabolism in *C. elegans* (Lapierre et al. 2013), mammals (Singh et al. 2009) as well as in yeast

(van Zutphen et al. 2014). Similarly in *Drosophila*, which has two perilipins (*plin1* and *plin2*), the double mutants are viable but have small lipid droplets. This suggests that perilipins are required for growth or maintenance of lipid droplets, but are dispensable for lipolysis (Bi et al. 2012). The abnormal LD behavior, but viability, of W01A8.1 null animals suggests a similar regulatory role for the nematode perilipin-related protein in the regulation of fat metabolism.

Our results suggest that the previously accepted view of a perilipin-independent nematode fatty acid flux of LDs needs to be revisited. Clearly we see evidence for perilipin-like LD regulation that is evolutionarily conserved (Fig. 5). With only a single gene and a toolbox of forward and reverse genetic approaches at hand, *C. elegans* offers an opportunity to explore the exact role of perilipin-related factors in fat regulation throughout development of many different somatic and germline cells. Exploitation of these opportunities will likely reveal new levels of regulation and novel players in the complex and vital regulation of fat in all organisms.

Acknowledgements

Authors thank WormBase and NCBI for accessibility of data.

References

Altschul SF, Madden TL, Schaffer AA, Zhang J, Zhang Z, Miller W and Lipman DJ. 1997. Gapped BLAST and PSI-BLAST: a new generation of protein database search programs. *Nucleic Acids Res* **25**: 3389-402.

Barros AG, Liu J, Lemieux GA, Mullaney BC and Ashrafi K. 2012. Analyses of C. elegans fat metabolic pathways. *Methods Cell Biol* **107**: 383-407.

Bi J, Xiang Y, Chen H, Liu Z, Gronke S, Kuhnlein RP and Huang X. 2012. Opposite and redundant roles of the two Drosophila perilipins in lipid mobilization. *J Cell Sci* **125**: 3568-77.

Biegert A and Soding J. 2008. De novo identification of highly diverged protein repeats by probabilistic consistency. *Bioinformatics* **24**: 807-14.

Birney E, Clamp M and Durbin R. 2004. GeneWise and Genomewise. *Genome Res* **14**: 988-95.

Birsoy K, Festuccia WT and Laplante M. 2013. A comparative perspective on lipid storage in animals. *J Cell Sci* **126**: 1541-52.

Brasaemle DL. 2007. Thematic review series: adipocyte biology. The perilipin family of structural lipid droplet proteins: stabilization of lipid droplets and control of lipolysis. *J Lipid Res* **48**: 2547-59.

Brasaemle DL, Dolios G, Shapiro L and Wang R. 2004. Proteomic analysis of proteins associated with lipid droplets of basal and lipolytically stimulated 3T3-L1 adipocytes. *J Biol Chem* **279**: 46835-42.

Brenner S. 1974. The genetics of Caenorhabditis elegans. *Genetics* **77**: 71-94.

Dai Z, Qi W, Li C, Lu J, Mao Y, Yao Y, Li L, Zhang T, Hong H, Li S, Zhou T, Yang Z, Yang X, Gao G and Cai W. 2013. Dual regulation of adipose triglyceride lipase by pigment epithelium-derived factor: a novel mechanistic insight into progressive obesity. *Mol Cell Endocrinol* **377**: 123-34.

Dickinson DJ, Ward JD, Reiner DJ and Goldstein B. 2013. Engineering the Caenorhabditis elegans genome using Cas9-triggered homologous recombination. *Nat Methods* **10**: 1028-34.

Du X, Barisch C, Paschke P, Herrfurth C, Bertinetti O, Pawolleck N, Otto H, Ruhling H, Feussner I, Herberg FW and Maniak M. 2013. Dictyostelium lipid droplets host novel proteins. *Eukaryot Cell* **12**: 1517-29.

Hickenbottom SJ, Kimmel AR, Londos C and Hurley JH. 2004. Structure of a lipid droplet protein; the PAT family member TIP47. *Structure* **12**: 1199-207.

Kimmel AR, Brasaemle DL, McAndrews-Hill M, Sztalryd C and Londos C. 2010. Adoption of PERILIPIN as a unifying nomenclature for the mammalian PAT-family of intracellular lipid storage droplet proteins. *J Lipid Res* **51**: 468-71.

Lapierre LR, Silvestrini MJ, Nunez L, Ames K, Wong S, Le TT, Hansen M and Melendez A. 2013. Autophagy genes are required for normal lipid levels in C. elegans. *Autophagy* **9**: 278-86.

Lass A, Zimmermann R, Oberer M and Zechner R. 2011. Lipolysis - a highly regulated multi-enzyme complex mediates the catabolism of cellular fat stores. *Prog Lipid Res* **50**: 14-27.

Lee JH, Kong J, Jang JY, Han JS, Yul J, Lee J and Kim JB. 2014. Lipid droplet protein LID-1 mediates ATGL-1-dependent lipolysis during fasting in Caenorhabditis elegans. *Mol Cell Biol*.

Liu Z, Li X, Ge Q, Ding M and Huang X. 2014. A lipid droplet-associated GFP reporter-based screen identifies new fat storage regulators in C. elegans. *J Genet Genomics* **41**: 305-13.

Lu X, Gruia-Gray J, Copeland NG, Gilbert DJ, Jenkins NA, Londos C and Kimmel AR. 2001. The murine perilipin gene: the lipid droplet-associated perilipins derive from tissue-specific, mRNA splice variants and define a gene family of ancient origin. *Mamm Genome* **12**: 741-9.

Notredame C, Higgins DG and Heringa J. 2000. T-Coffee: A novel method for fast and accurate multiple sequence alignment. *J Mol Biol* **302**: 205-17.
O'Rourke EJ and Ruvkun G. 2013. MXL-3 and HLH-30 transcriptionally link lipolysis and autophagy to nutrient availability. *Nat Cell Biol* **15**: 668-76.
O'Rourke EJ, Soukas AA, Carr CE and Ruvkun G. 2009. C. elegans major fats are stored in vesicles distinct from lysosome-related organelles. *Cell Metab* **10**: 430-5.
Punta M, Coggill PC, Eberhardt RY, Mistry J, Tate J, Boursnell C, Pang N, Forslund K, Ceric G, Clements J, Heger A, Holm L, Sonnhammer EL, Eddy SR, Bateman A and Finn RD. 2012. The Pfam protein families database. *Nucleic Acids Res* **40**: D290-301.
Remmert M, Biegert A, Hauser A and Soding J. 2011. HHblits: lightning-fast iterative protein sequence searching by HMM-HMM alignment. *Nat Methods* **9**: 173-5.
Schweiger M, Schreiber R, Haemmerle G, Lass A, Fledelius C, Jacobsen P, Tornqvist H, Zechner R and Zimmermann R. 2006. Adipose triglyceride lipase and hormone-sensitive lipase are the major enzymes in adipose tissue triacylglycerol catabolism. *J Biol Chem* **281**: 40236-41.
Shen WJ, Patel S, Miyoshi H, Greenberg AS and Kraemer FB. 2009. Functional interaction of hormone-sensitive lipase and perilipin in lipolysis. *J Lipid Res* **50**: 2306-13.
Simeckova K, Brozova E, Vohanka J, Pohludka M, Kostrouch Z, Krause MW, Rall JE and Kostrouchova M. 2007. Supplementary nuclear receptor NHR-60 is required for normal embryonic and early larval development of Caenorhabditis elegans. *Folia Biol (Praha)* **53**: 85-96.
Singh R, Kaushik S, Wang Y, Xiang Y, Novak I, Komatsu M, Tanaka K, Cuervo AM and Czaja MJ. 2009. Autophagy regulates lipid metabolism. *Nature* **458**: 1131-5.
Tabara H, Sarkissian M, Kelly WG, Fleenor J, Grishok A, Timmons L, Fire A and Mello CC. 1999. The rde-1 gene, RNA interference, and transposon silencing in C. elegans. *Cell* **99**: 123-32.
Teixeira L, Rabouille C, Rorth P, Ephrussi A and Vanzo NF. 2003. Drosophila Perilipin/ADRP homologue Lsd2 regulates lipid metabolism. *Mech Dev* **120**: 1071-81.
Timmons L, Court DL and Fire A. 2001. Ingestion of bacterially expressed dsRNAs can produce specific and potent genetic interference in Caenorhabditis elegans. *Gene* **263**: 103-12.
van Zutphen T, Todde V, de Boer R, Kreim M, Hofbauer HF, Wolinski H, Veenhuis M, van der Klei IJ and Kohlwein SD. 2014. Lipid droplet autophagy in the yeast Saccharomyces cerevisiae. *Mol Biol Cell* **25**: 290-301.
Vohanka J, Simeckova K, Machalova E, Behensky F, Krause MW, Kostrouch Z and Kostrouchova M. 2010. Diversification of fasting regulated transcription in a cluster of duplicated nuclear hormone receptors in C. elegans. *Gene Expr Patterns* **10**: 227-36.
Wang C and St Leger RJ. 2007. The Metarhizium anisopliae Perilipin Homolog MPL1 Regulates Lipid Metabolism, Appressorial Turgor Pressure, and Virulence. *J Biol Chem* **282**: 21110-5.
Zhang P, Na H, Liu Z, Zhang S, Xue P, Chen Y, Pu J, Peng G, Huang X, Yang F, Xie Z, Xu T, Xu P, Ou G, Zhang SO and Liu P. 2012. Proteomic study and marker protein identification of Caenorhabditis elegans lipid droplets. *Mol Cell Proteomics* **11**: 317-28.

483

Figure 1(on next page)

Identification of *C. elegans* protein W01A8.1a as a close homologue of vertebrate perilipin.

C. elegans protein W01A8.1a is compared with nematode homologues of pairwise sequence identity lower then 70% and with Plin2 and 3 from two diverse vertebrates. The three perilipin specific domains (indicated in red) were identified through homology with human Plin3. The six 11-mer repeats in W01A8.1a (positions 126-136, 137-147, 148-158, 159-169, 170-180 and 181-191) were established with HHrepID algorithm (Biegert & Soding 2008). The N-terminal PAT domain is thought to interact with HSL. The central domain consisting of imperfect 11-mer repeats forming amphipathic helices is responsible for the main affinity to LDs and the C-terminal domain containing an apolipoprotein-like 4-helix bundle probably plays an additional role in the affinity to LDs and is known to interact with ABHD5 in mammalian Plin1 and 3 (Brasaemle 2007). Alignment was done using T-coffee alignment of all available nematode sequences aligned with vertebrate Plin2 and 3 sequences in three iterations using ProfileAlign routine in MyHits suite (myhits.isb-sib.ch). Selected sequences from top to bottom: (Species, database identifier): *Caenorhabditis elegans*, Q23095; *Strongyloides ratti*, CACX01001972.1; *Loa loa*, E1G5Y0 and ADBU02007219.1; *Haemonchus contortus*, CDJ80228.1; *Bursaphelenchus xylophilus*, CADV01008520.1; *Heterorhabditis bacteriophora*, ES742365.1 and ACKM01001830.1; *Ascaris suum*, U1NU60; *Homo sapiens* 2, PLIN2_HUMAN; *Homo sapiens* 3, PLIN3_HUMAN; *Latimeria chalumnae* 2, H3AYC0; *Latimeria chalumnae* 3, GAAA01019375.1. Nucleotide sequences were translated with Wise2 program (Birney, Clamp & Durbin 2004). Amino acid types are colored according to the Clustal scheme (jalview.org/help/html/colourSchemes/clustal.html).

```
Q23095_CAEEL   31 AYTKTKEFHPLLNSTLNSAEEKVSTVGNYA---AQKAYDGYNSYYVKPKNTAYEAVSYGTERA  90
PLIN1_HUMAN    40 TYTSTKEAHPLVASVCNAYEKGVQSASSLAAWSMEPVVRRLSTQFTAANELACRGLDHLEEKI 102
PLIN2_HUMAN    32 AYLSTKDQYPYLKSVCEMAENGVKTITSVAMTSALPIIQKLEPQIAVANTYACKGLDRIEERL  94
PLIN3_HUMAN    45 AYASTKESYPHIKTVCDAAEKGVRTLTAAAVSGAQPILSKLEPQIASASEYAHRGLDKLEENL 107
PLIN5_HUMAN    42 VYSAAKDRHPLLGSACRLAENCVCGLTTRALDHAQPLLEHLQPQLATMNSLACRGLDKLEEKL 104

Q23095_CAEEL   91 KTAVESGKQAAIVGGTFGIGAAVVLTQFSLALSAGGAALVLEQVDSAKKLGSSAISTIKEAEL 153
PLIN1_HUMAN   103 PALQYPPEKIASELKDTISTRLRSAR-------NSISVPIASTSDKVLGAALAGCELAWGVAR 158
PLIN2_HUMAN    95 PILNQPSTQIVANAKGAVTGAKDAVTTTVTGAKDSVASTITGVMDKTKGAVTGSVEKTKSVVS 157
PLIN3_HUMAN   108 PILQQPTEKVLADTKELVSSKVSGAQEMVSSAKDTVATQLSEAVDATRGAVQSGVDKTKSVVT 170
PLIN5_HUMAN   105 PFLQQPSETVVTSAKDVV-------------------ASSVTGVVDLARRGRRWSVELKRS--- 146

Q23095_CAEEL   154 AVEHRIFSA-LHQAQRIAMVPVEKITENTNSLL-----DILDGAVQKGLNIEVPPSVNLTIGQ 210
PLIN1_HUMAN    159 DTAEFAANTRAGRLASGGADLALGSIEKVVEYLLPPDKEESAPAPGHQQ-----AQKSPKAKP 216
PLIN2_HUMAN    158 GSINTVLGSRMMQLVSSGVENALTKSELLVEQYLPLTEEELEKEAKKVEGFDL------VQKP 214
PLIN3_HUMAN    171 GGVQSVMGSRLGQMVLSGVDTVLGKSEEWADNHLPLTDAELARIATSLDGFDVASVQQQRQEQ 233
PLIN5_HUMAN    147 ----------VSHAVDVVLEKSEELVDHFLPMTEEELAALAAEAEGPEVGSVEDQRRQQ 195

Q23095_CAEEL   211 RVKNLASLIVQGVSNKAHDHVIDPINE---RARNYLEQLSQSFVLLD----IVR---EKKTWV 263
PLIN1_HUMAN    217 SLLSRVGALTNTL----SRYTVQTMARALEQGHTVAMWIPGVVPLSSLAQWGAS---VAMQAV 272
PLIN2_HUMAN    215 SYYVRLGSLSTKLHSRAYQQALSRVKEAKQKSQQTISQLHSTVHLIEFARKNVYSANQKIQDA 277
PLIN3_HUMAN    234 SYFVRLGSLSERLRQHAYEHSLGKLRATKQRAQEALLQLSQVLSLMETVKQGVD---QKLVEG 293
PLIN5_HUMAN    196 GYFVRLGSLSARIRHLAYEHSVGKLRQSKHRAQDTLAQLQETLELIDHMQCGVT---PTAPAC 255

Q23095_CAEEL   264 IEKSNELSTSVFDFKKTLEEEAQKYKVAPEEMLMKHIQ----------STSEQLSTQLQSLREK 317
PLIN1_HUMAN    273 SRRRSEVRVPWLHSLAAAQEEDHEDQTDTEGEDTEEEEELETEENKFSEVAALPGPRGLLGGV 335
PLIN2_HUMAN    278 QDKLYLSWVEWKRSIGYDDTDESHCAEHIESRTLAIAR----------NLTQQLQTTCHTLLSN 331
PLIN3_HUMAN    294 QEKLHQMWLSWNQKQLQGPEKEPPKPEQVESRALTMFR----------DIAQQLQATCTSLGSS 347
PLIN5_HUMAN    256 PGKVHELWGEWGQRPPESRRRSQA-----ELETLVLSR----------SLTQELQGTVEALESS 304

Q23095_CAEEL   318 GQNVFGD-GTKIDSTIDYLENLKKNFTDAEDVYKVRDEVLNEGRQR--IAELSTWTTSLL 374
PLIN1_HUMAN    336 AHTLQKTLQTTISAVTWAPAAVLGMAGRVLHLTPAPAVSSTKGRAMSLSDALKGVTDNVV 395
PLIN2_HUMAN    332 IQGVPQNIQDQAKHMGVMAGDIYSVFRNAASFKEVSDSLLTSSKGQ--LQKMKESLDDVM 389
PLIN3_HUMAN    348 IQGLPTNVKDQVQQARRQVEDLQATFSSIHSFQDLSSSILAQSRER--VASAREALDHMV 405
PLIN5_HUMAN    305 VRGLPAGAQEKVAELVRRSVDALQTAFADARCFRDVPAAALAEGRGR--VAHAHACVDELL 362
```

2

The expression *W01A8.1::gfp* reporter genes in transgenic strains.

W01A8.1a/c::GFP is shown in A, C, E, G, and I, and corresponding areas in Nomarski optics are shown in B, D, F, H and J. A) The onset of expression of W01A8.1a/c::GFP in epidermal cells and in intestinal cells of three-fold embryo. C) The expression of W01A8.1a/c::GFP in intestinal cells of an L2 larva. E and G) W01A8.1a/c::GFP expression in epidermal cells and intestinal cells of a young adult hermaphrodite. G) shows detail of the GFP fluorescence around lipid droplet-like structures in the intestine that are marked by arrows and arrowheads. Corresponding image in Nomarski optics is in H. I) shows in higher magnification the lipid droplet-like structures in epidermal cells labeled by W01A8.1a/c::GFP (shown in Nomarski optics in the J). K) shows lipid droplets of an unfixed intestine labeled by W01A8.1b::GFP (corresponding Nomarski image is in L). M, N and O) show part of the intestine of an adult larva expressing W01A8.1b::GFP (M) with corresponding staining of lipid droplets by LipidTox (N). O) shows the LipidTox positive lipid droplets (red) with W01A8.1b::GFP on the periphery (green) in a detail of a merged view. Bars represent 50 µm in B, H, J, L and N and 100 µm in D and F.

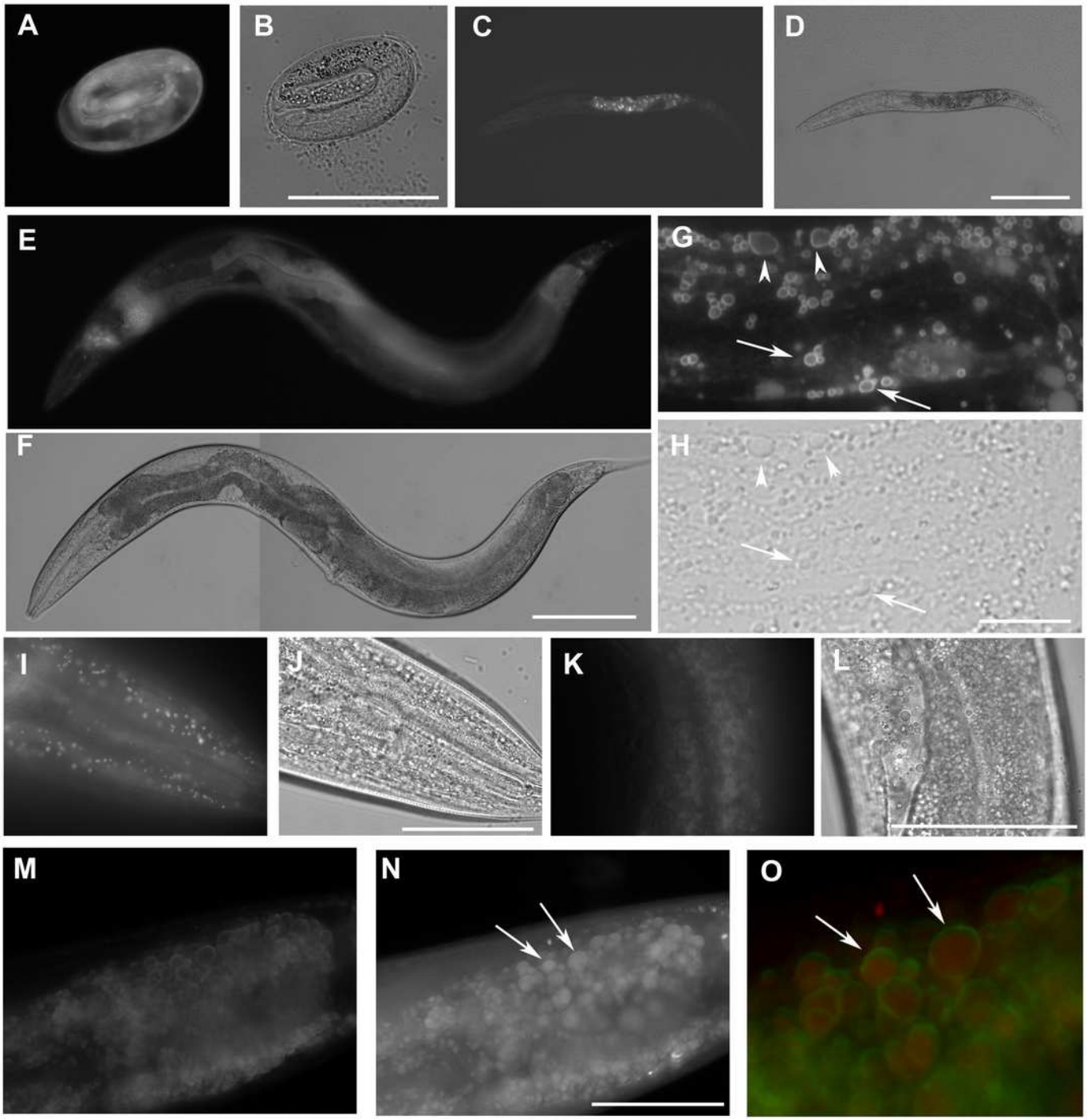

3

Expression of human perilipins fused to GFP in *C. elegans*.

A, B and C show expression of human PLIN1::GFP in live transgenic *C. elegans*. PLIN1::GFP is localized on vesicles with an appearance of lipid droplets. PLIN2::GFP (D, E and F) is localized in transgenic animals on vesicular structures with an appearance of lipid droplets similarly as PLIN1::GFP. PLIN3::GFP (G, H and I) yields a more diffuse cytoplasmic pattern with faintly stained vesicular structures. A, D and G and details in C, F and I show GFP in fluorescence microscopy and B, E and H corresponding areas to A, D and G in Nomarski optics. J, K and L show PLIN2::GFP in fluorescence microscopy (J) in fixed *C. elegans* stained with LipidTox (K). The area indicated by the white rectangle in J and K is magnified and merged for co-localization of PLIN2::GFP (green) and LipidTox (red) in L. Arrows indicate lipid droplets clearly marked by GFP with the LipidTox positive content. Bars represent 50 µm.

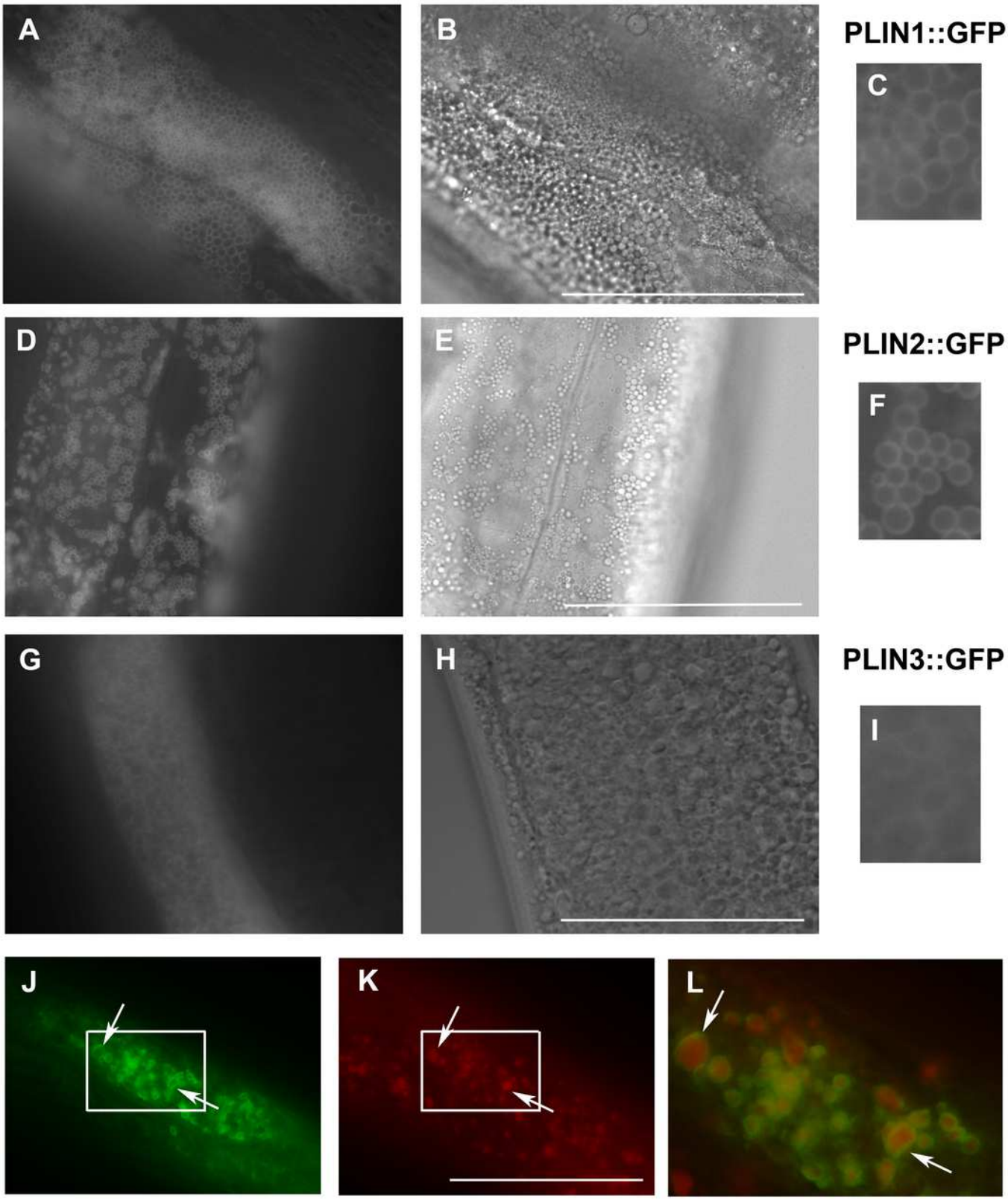

4

Loss of *W01A8.1* function results in abnormal lipid droplet appearance.

A and B show an embryo of a hermaphrodite inhibited for *W01A8.1* function by RNAi. Large lipid droplets stained by LipidTox (B) are visible also in Nomarski optics (A) in contrast with a control embryo which has only small and more evenly distributed lipid droplets (C - Nomarski optics and D - LipidTox staining). E to J and L and M show structures observed in animals with disrupted *W01A8.1*. E and F show structures with the appearance of lipid droplets in the intestine of an animal with disrupted W01A8.1 balanced with the synthetic transgene *W01A8.1(synth)::gfp*. GFP tagged synthetic W01A8.1a is localized on lipid droplets-like vesicular structures (E). F shows the same area stained with Lipidtox. G shows in magnification a merged image of the area indicated by white rectangles in E and F. |Arrows indicate W01A8.1(synth)::GFP labeled lipid droplets (green) positive for lipids in LipidTox staining (red). H and I show an embryo of a parent with disrupted W01A8.1 that had confirmed loss of the balancing transgene. Large LipidTox stained droplets are visible in Nomarski optics (H) as well as in LipidTox staining (I). J and K are taken from video recorded focal planes of live animals. J shows an embryo with disrupted *W01A8.1* and confirmed loss of the balancing transgene. Large vesicular structures are formed around the dividing nucleus (arrows). K shows a control embryo with normal appearance of the nuclear periphery (arrow). L and M show a one cell embryo from a parent with disrupted *W01A8.1* and confirmed loss of extrachromosomal array after fixation and staining by LipidTox with large lipid droplets around the dividing nucleus visible in Nomarski optics (L) and positive for lipids in Lipidtox staining (K) indicated by arrows). Bars represent 10 µm.

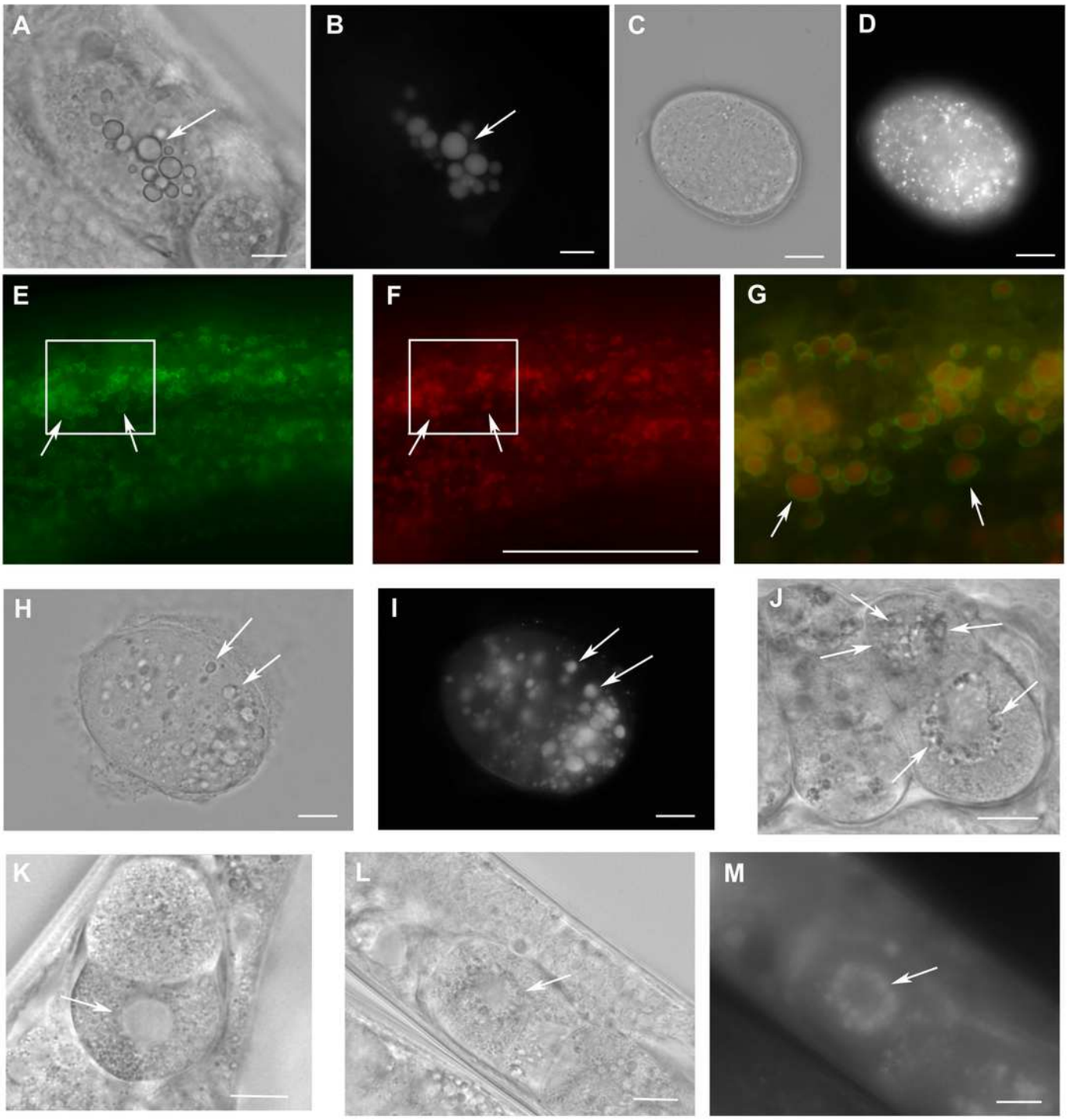

Figure 5(on next page)

Enzymes and regulatory proteins involved in lipolysis (Adapted from (Lass et al. 20114).

Mammalian proteins are indicated above the arrows and their *C.elegans* orthologues (Lee et al. 2014) below. Triacylglycerol (TAG) is progressively hydrolysed to diacylglycerol (DAG), monoacylglycerol (MAG) and glycerol (G) by lipases specific for each of these steps: adipose triacylglycerol lipase (ATGL), hormone-sensitive lipase (HSL) and finally monoacylglycerol lipase (MGL). HSL also shows some activity in the first and third step. The access of ATGL and HSL to lipid droplets is regulated by perilipin, which is under the control of protein kinase A (PKA). W01A8.1 is established as perilipin orthologue in the present work. For more details see Discussion.

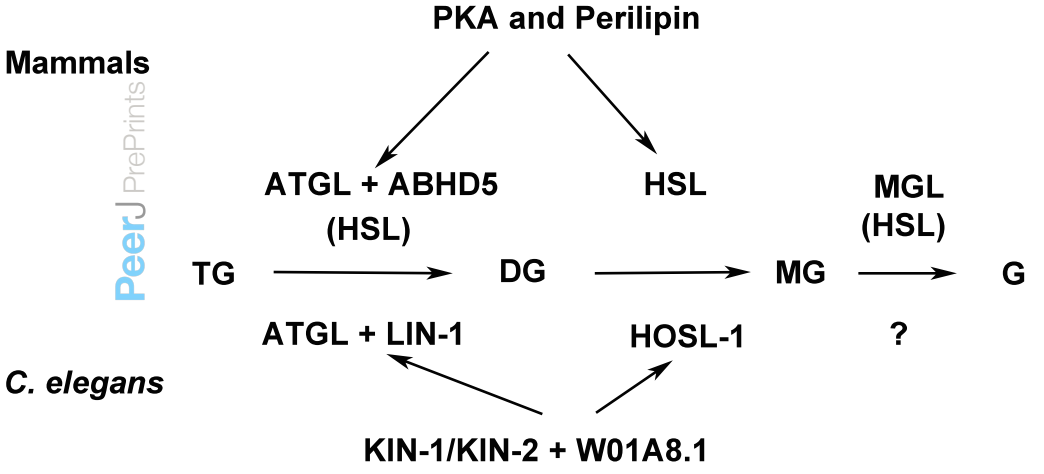

PeerJ PrePrints | https://dx.doi.org/10.7287/peerj.preprints.904v1 | CC-BY 3.0 Open Access | rec: 17 Mar 2015, publ: 17 Mar 2015